Nonlinear Dyn (2012) 69:193–210
DOI 10.1007/s11071-011-0257-2

ORIGINAL PAPER

Stability and bifurcations of an axially moving beam with an intermediate spring support

Mergen H. Ghayesh

Received: 30 June 2011 / Accepted: 19 October 2011 / Published online: 10 November 2011

Abstract The forced non-linear vibrations of an axially moving beam fitted with an intra-span spring-support are investigated numerically in this paper. The equation of motion is obtained via Hamilton's principle and constitutive relations. This equation is then discretized via the Galerkin method using the eigenfunctions of a hinged-hinged beam as appropriate basis functions. The resultant non-linear ordinary differential equations are then solved via either the pseudo-arclength continuation technique or direct time integration. The sub-critical response is examined when the excitation frequency is set near the first natural frequency for both the systems with and without internal resonances. Bifurcation diagrams of Poincaré maps obtained from direct time integration are presented as either the forcing amplitude or the axial speed is varied; as we shall see, a sequence of higher-order bifurcations ensues, involving periodic, quasi-periodic, periodic-doubling, and chaotic motions.

Keywords Axially moving beams · Non-linear dynamics · Stability

M.H. Ghayesh (✉)
Department of Mechanical Engineering, McGill University, Montreal, Quebec, Canada H3A 2K6
e-mail: mergen.hajghayesh@mail.mcgill.ca

1 Introduction

The class of axially moving systems are present in many technological devices and machines components. Many examples of these types of systems, such as textile fibres, paper sheets, band saw blades, magnetic tapes, robotic manipulators, and oil pipelines can be found in civil, mechanical, aerospace, and automotive applications. Most often, this class of the systems is modelled as either an axially moving string or beam, which is categorised as gyroscopic systems.

The dynamics of these systems is greatly affected by the axial speed. This feature is responsible for the existence of complex mode functions by preventing standing (stationary) flexural waves, and arising travelling-waves. At a certain axial speed, known as *critical speed*, the first natural frequency of a conservative system vanishes and the stability is lost by a divergence. The early studies on the dynamics of axially moving systems [1, 2] focused on the linear aspects of the problems, thus mainly on the critical speed for buckling, natural frequencies, and complex mode functions.

Beyond the first instability, the amplitude of the vibrations or static divergence is large, and hence the validity of linear theory diminishes [3]. Moreover, most post-critical bifurcations occur over non-trivial states (attractors), and can be reliably predicted via non-linear models. The early studies on this topic by Mote [3], Naguleswaran and Williams [4], Thurman and Mote [5], Shih [6], Simpson [7], and Holmes [8],

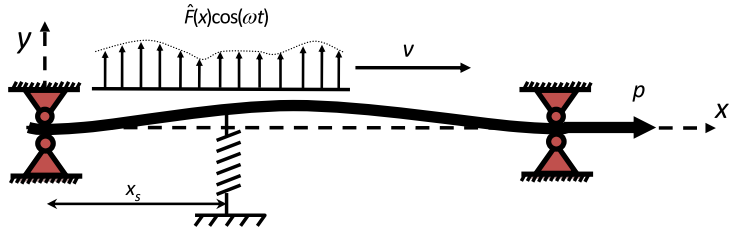

Fig. 1 Schematic representation of a hinged-hinged axially moving beam, additionally supported by a non-linear spring

for example, considered string and beam models of the system employing analytic, experimental, and energetic approaches.

Soon after, in the 1990s, more complete models of the system started appearing, notably by Wickert and Mote [9, 10], Wickert [11], Pakdemirli and co-workers [12–15], Yuh and Young [16], Zhu and Guo [17], Chakraborty and Mallik [18], Zhang and Zu [19], and Tan et al. [20]. In a fundamental work by Wickert and Mote [9], for example, the free and forced dynamics of a linear axially moving continuum was investigated via the eigenfunction method. This study was followed and extended in [10] using the Green function method, and in [11] considering both sub- and super-critical speed regimes. Also, in a series of papers by Pakdemirli and co-workers [12–15], a systematic research on this topic was conducted using some perturbation techniques.

Later, these studies were extended by Marynowski and co-investigators [21–25], who considered several dissipation mechanisms; Chen and co-workers [26–35], who considered string and different beam models via different analytical and numerical methods; Pellicano and Vestroni [36]; Suweken and Van Horssen [37]; and Huang et al. [38]. Recently, in a series of papers by the author and co-workers [39–50], the vibration and stability of axially moving systems were examined. Specifically, these analyses included several system models: linear, non-linear, energy dissipative, laminated, Euler–Bernoulli, Rayleigh, and Timoshenko models.

In this paper, a hinged-hinged axially moving beam, additionally supported by a non-linear spring [51–54] and subjected to a distributed harmonic excitation, is considered. The non-linear equation of motion is derived using Hamilton's principle and discretized via Galerkin's technique. The pseudo-arclength continuation technique [55], along with variable step-size Runge–Kutta method, are employed to solve the resultant non-linear ordinary differential

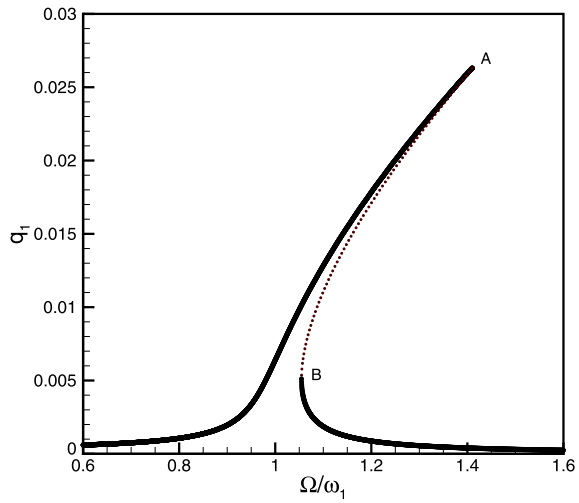

Fig. 2 The amplitude-frequency response of the system with no internal resonances in the driven mode. *Bold line* and *dotted lines* represent the stable and unstable solutions, respectively

equations. The amplitude-frequency response of the system, as well as bifurcation diagrams of the Poincaré maps, are obtained, and the attention is focused mainly on the role of the spring stiffness and location. The analysis also includes the cases with a three-to-one internal resonance. The results are illustrated in the form of bifurcation diagrams of Poincaré maps and amplitude-frequency responses.

2 Equation of motion

Shown in Fig. 1 is a general axially moving beam of length L, with constant density ρ, area moment of inertia I, cross-sectional area A, and Young's modulus E, which is travelling at a constant axial speed v. Furthermore, the beam is subjected to a pretension p and a distributed transverse force $\hat{F}(x,t) = \hat{F}(x)\cos(\omega t)$ per unit length along the entire span. A spring, with linear and non-linear stiffness coefficients of k_1 and k_2

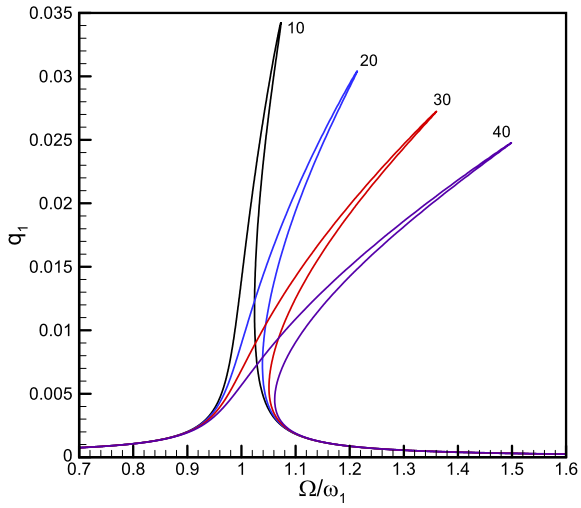

Fig. 3 The amplitude-frequency response of the system with no internal resonances in the driven mode for several non-linearity coefficients v_1. The v_1 values are indicated on the curves; $c = 0.2$, $v_f = 0.173$, $\mu = 0.04$, $f_1 = 0.0055$, $f_i = 0$ $(i = 2, 3, 4, 5, 6)$, $\alpha = 1.5$, $\gamma = 0.3$, $\xi_s = 0.3$

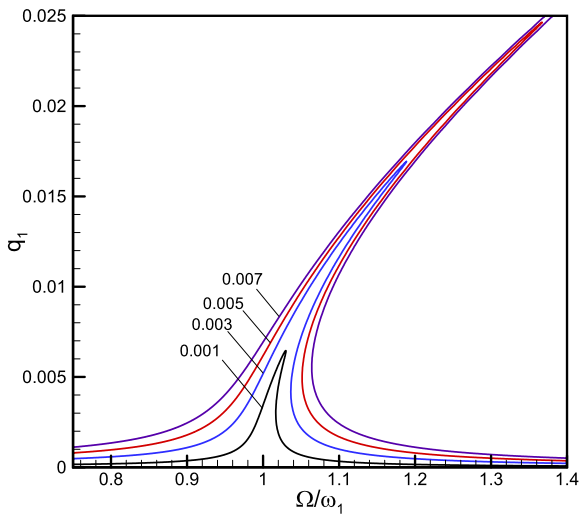

Fig. 4 The amplitude-frequency response of the system with no internal resonances in the driven mode for several values of the forcing amplitude. The f_1 values are indicated on the curves; $c = 0.2$, $v_f = 0.173$, $v_1 = 33.526$, $\mu = 0.04$, $f_i = 0$ $(i = 2, 3, 4, 5, 6)$, $\alpha = 1.5$, $\gamma = 0.3$, $\xi_s = 0.3$

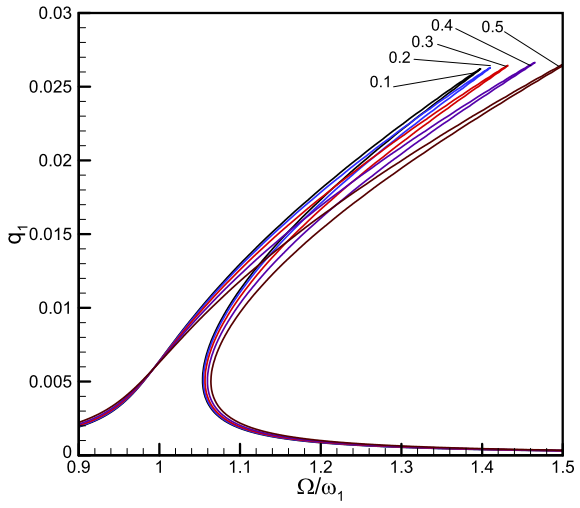

Fig. 5 The amplitude-frequency response of the system with no internal resonances in the driven mode for several axial speeds. The c values are indicated on the curves; $v_f = 0.173$, $v_1 = 33.526$, $\mu = 0.04$, $f_1 = 0.0055$, $f_i = 0$ $(i = 2, 3, 4, 5, 6)$, $\alpha = 1.5$, $\gamma = 0.3$, $\xi_s = 0.3$

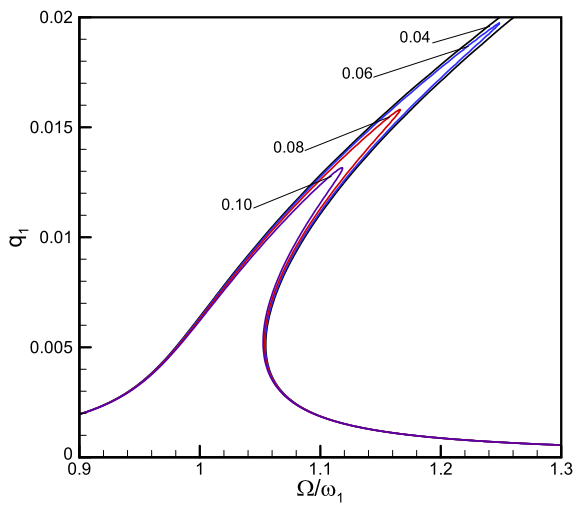

Fig. 6 The amplitude-frequency response of the system with no internal resonances in the driven mode for several damping coefficients. The μ values are indicated on the curves. $c = 0.2$, $v_f = 0.173$, $v_1 = 33.526$, $f_1 = 0.0055$, $f_i = 0$ $(i = 2, 3, 4, 5, 6)$, $\alpha = 1.5$, $\gamma = 0.3$, $\xi_s = 0.3$

respectively, is attached at a distance x_s from the left end of the beam.

The equation of motion is obtained under the following assumptions: (i) the system is modelled as a non-linear Euler–Bernoulli beam, i.e., rotary inertia and shear deformation are neglected; (ii) the beam has a uniform cross-sectional area; (iii) the type of non-linearity is geometric; (iv) the source of non-linearity in the beam model is due to the stretching effect of the mid-plane of the beam; (v) the equation is truncated at third order; (vi) the spring is assumed to be attached to

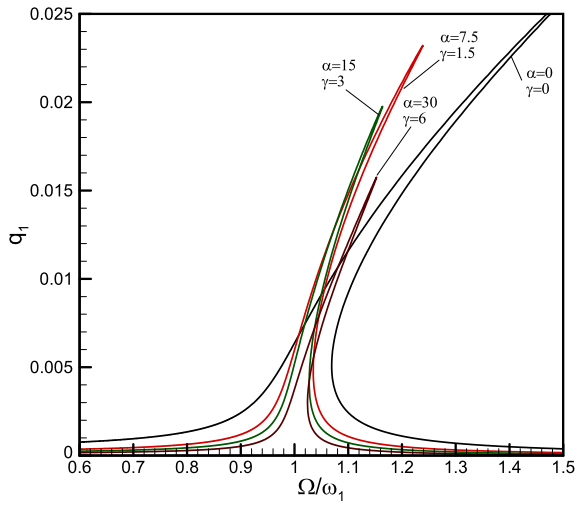

Fig. 7 The amplitude-frequency response of the system with no internal resonances in the driven mode for several stiffness coefficients of the spring. The α and γ values are indicated on the curves. $c = 0.4$, $v_f = 0.173$, $v_1 = 33.526$, $\mu = 0.04$, $f_1 = 0.0055$, $f_i = 0$ $(i = 2, 3, 4, 5, 6)$, $\xi_s = 0.4$

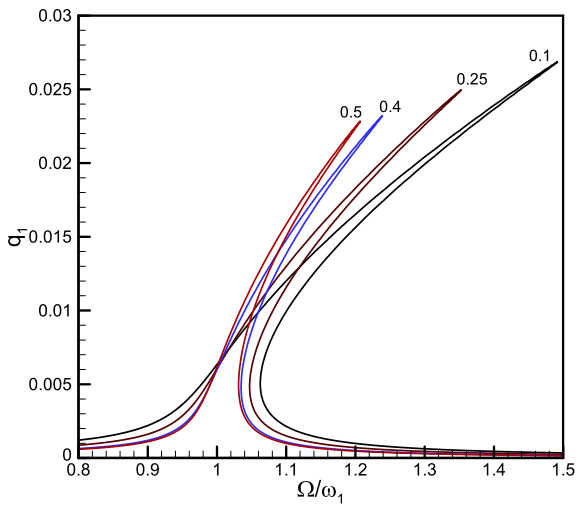

Fig. 8 The amplitude-frequency response of the system with no internal resonances in the driven mode for several spring locations. The ξ_s values are indicated on the curves. $c = 0.4$, $v_f = 0.173$, $v_1 = 33.526$, $\mu = 0.04$, $f_1 = 0.0055$, $f_i = 0$ $(i = 2, 3, 4, 5, 6)$, $\alpha = 7.5$, $\gamma = 1.5$

the centreline of the beam and its force is assumed to be purely in the transverse direction.

The potential energy of the system has three components: the strain energy of the beam π_b, of the nonlinear spring, π_s, and due to the pretension, π_p. The

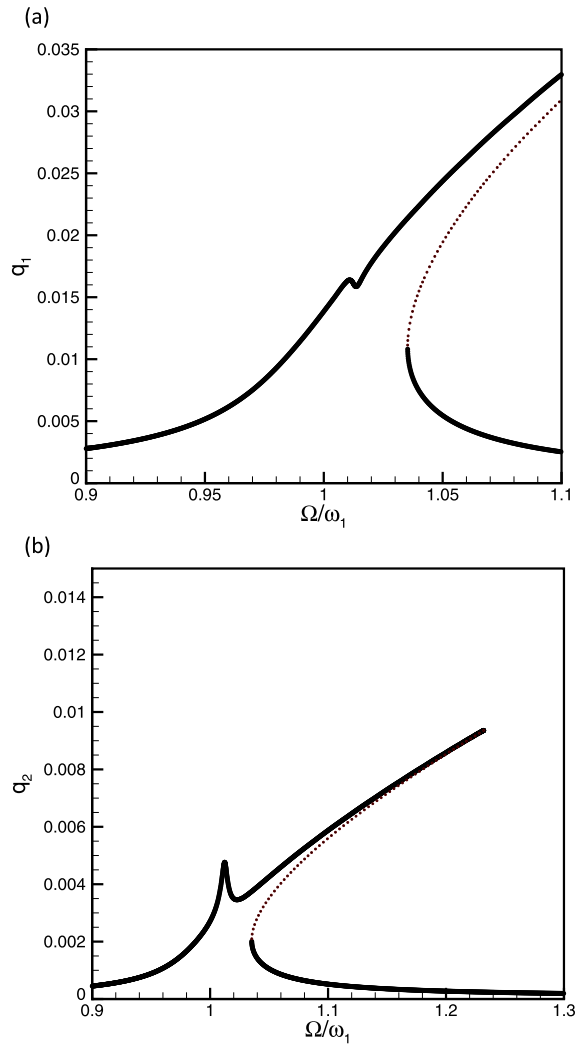

Fig. 9 The amplitude-frequency response of the system in the driven and companion modes possessing a three-to-one internal resonance, i.e., $\omega_2 \approx 3\omega_1$; (**a**) the amplitude of driven mode; (**b**) the amplitude of the second mode. *Bold line* and *dotted lines* represent the stable and unstable solutions, respectively

potential strain energy of the beam can be expressed as

$$\pi_\mathrm{b} = \frac{1}{2}EA\int_0^L \left[\frac{\partial u}{\partial x} + \frac{1}{2}\left(\frac{\partial w}{\partial x}\right)^2\right]^2 dx + \frac{1}{2}EI\int_0^L \left(\frac{\partial^2 w}{\partial x^2}\right)^2 dx, \quad (1)$$

where $u(x,t)$ and $w(x,t)$ are respectively the longitudinal and transverse displacements. The potential energy due to the spring force and the pretension is given by

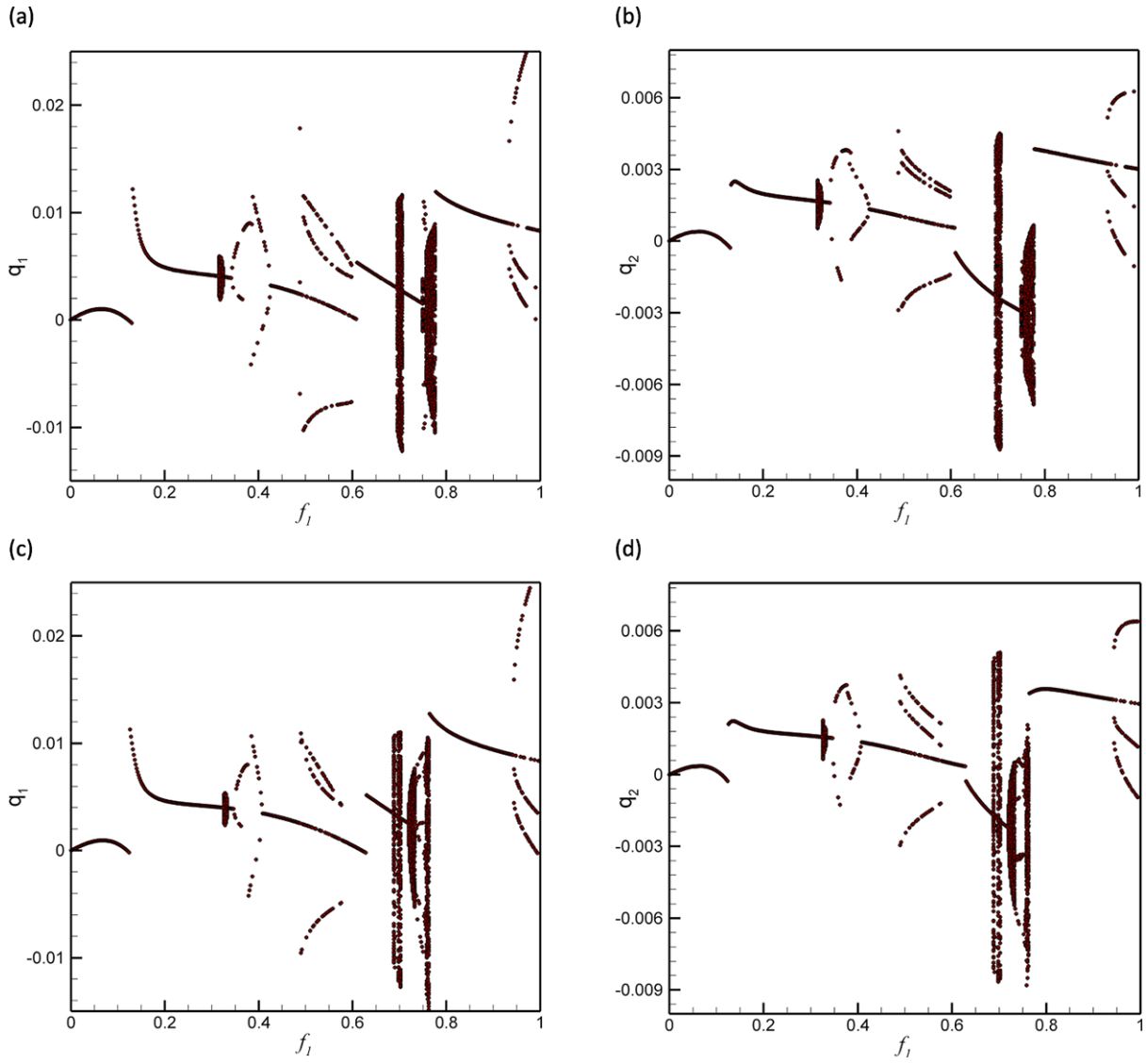

Fig. 10 Bifurcation diagrams of Poincaré points for increasing forcing amplitude on the system. The first and second modes, respectively, with (**a**, **b**) $\alpha = 0$ and $\gamma = 0$, (**c**, **d**) $\alpha = 0.6$ and $\gamma = 0.12$, (**e**, **f**) $\alpha = 1.5$ and $\gamma = 0.3$, (**g**, **h**) $\alpha = 3.0$ and $\gamma = 0.6$, (**i**, **j**) $\alpha = 5.0$ and $\gamma = 1.0$, (**k**, **l**) $\alpha = 7.5$ and $\gamma = 1.5$, and (**m**, **n**) $\alpha = 15$ and $\gamma = 3.0$. The axial speed is set to 0.7

$$\pi_s = \int_0^L \left(\frac{1}{2}k_1 w^2 + \frac{1}{4}k_2 w^4\right)\delta(x - x_s)\,dx, \tag{2}$$

$$\pi_p = p\int_0^L \left[\frac{\partial u}{\partial x} + \frac{1}{2}\left(\frac{\partial w}{\partial x}\right)^2\right]dx, \tag{3}$$

where $\delta(x)$ is the Dirac delta function; (2) implies that the restoring force of the spring is in the form $F = k_1 w + k_2 w^3$. The kinetic energy of the system can be expressed as follows:

$$T = \frac{1}{2}\rho A\int_0^L \left[\frac{\partial u}{\partial t} + v\left(1 + \frac{\partial u}{\partial x}\right)\right]^2 dx + \frac{1}{2}\rho A\int_0^L \left[\frac{\partial w}{\partial t} + v\frac{\partial w}{\partial x}\right]^2 dx. \tag{4}$$

The variation of the work done by the external distributed force on the beam can be expressed as

$$\delta W_F = \int_0^L \hat{F}(x)\cos(\omega t)\,\delta w\,dx. \tag{5}$$

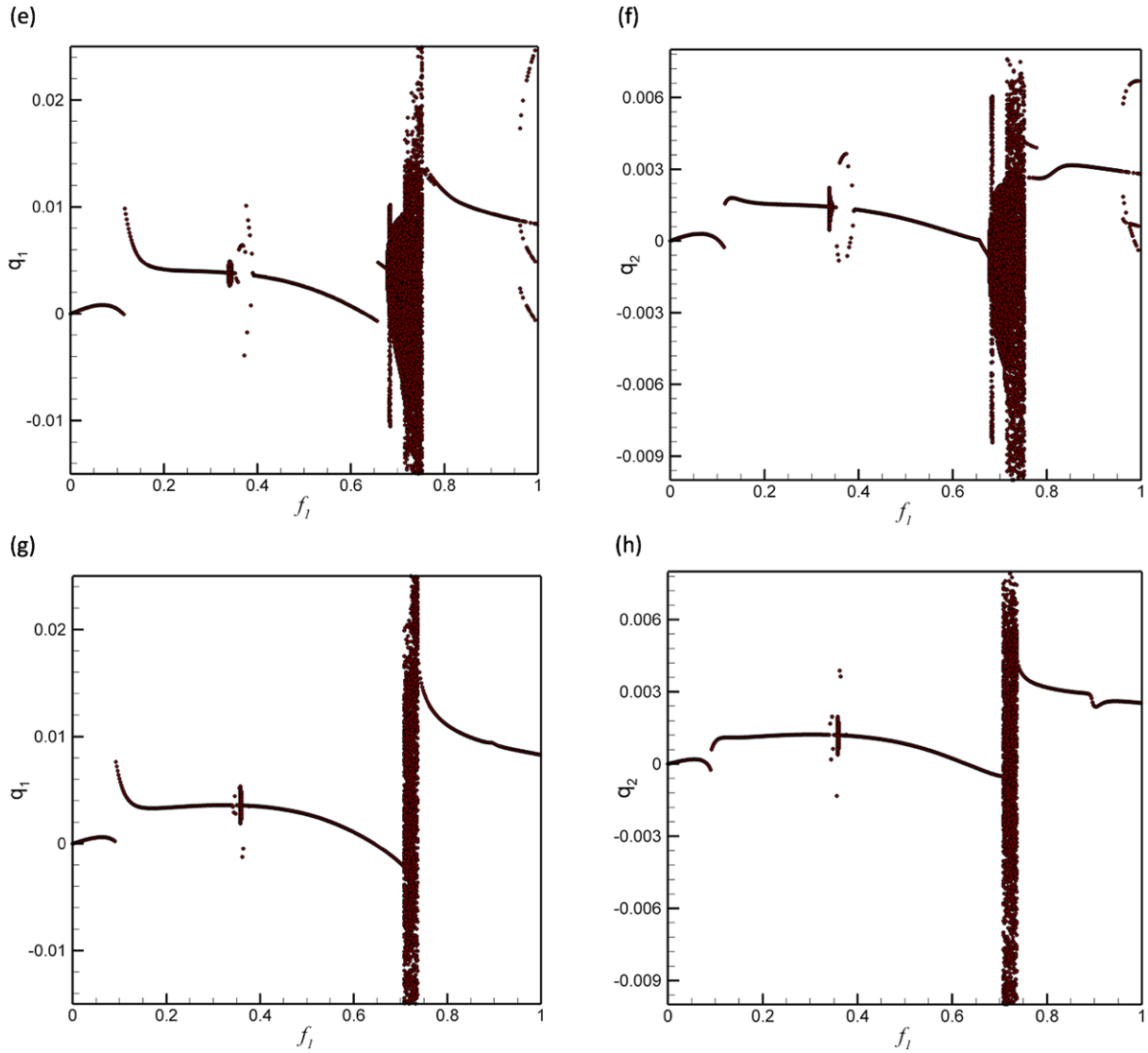

Fig. 10 (*Continued*)

The potential and kinetic energies for the beam and the spring-support, as well as the work done by the external force, can all be combined by inserting (1)–(5) into Hamilton's principle, which is given by

$$\delta \int_{t_1}^{t_2} \left(T - \pi_{\mathrm{b}} - \pi_{\mathrm{s}} - \pi_{\mathrm{p}}\right) dt + \int_{t_1}^{t_2} \delta W_F \, dt = 0. \quad (6)$$

This operation renders a large equation involving a double integral with limits from 0 to L and from t_1 to t_2. The variations δw and δu are arbitrary, which implies that the integrands should vanish. This generates the following equations of motion:

$$EA\left(\frac{\partial^2 u}{\partial x^2} + \frac{\partial^2 w}{\partial x^2}\frac{\partial w}{\partial x}\right) - \rho A\left(\frac{\partial^2 u}{\partial t^2} + 2v\frac{\partial^2 u}{\partial x \partial t} + v^2\frac{\partial^2 u}{\partial x^2}\right) = 0, \quad (7)$$

$$EA\left\{\frac{\partial^2 w}{\partial x^2}\left[\frac{\partial u}{\partial x} + \frac{1}{2}\left(\frac{\partial w}{\partial x}\right)^2\right] + \frac{\partial w}{\partial x}\left[\frac{\partial^2 u}{\partial x^2} + \frac{\partial^2 w}{\partial x^2}\frac{\partial w}{\partial x}\right]\right\} - EI\frac{\partial^4 w}{\partial x^4} - \delta\left(x - x_{\mathrm{s}}\right)\left(k_1 w + k_2 w^3\right) + p\frac{\partial^2 w}{\partial x^2} - \rho A\left(\frac{\partial^2 w}{\partial t^2} + 2v\frac{\partial^2 w}{\partial x \partial t} + v^2\frac{\partial^2 w}{\partial x^2}\right)$$

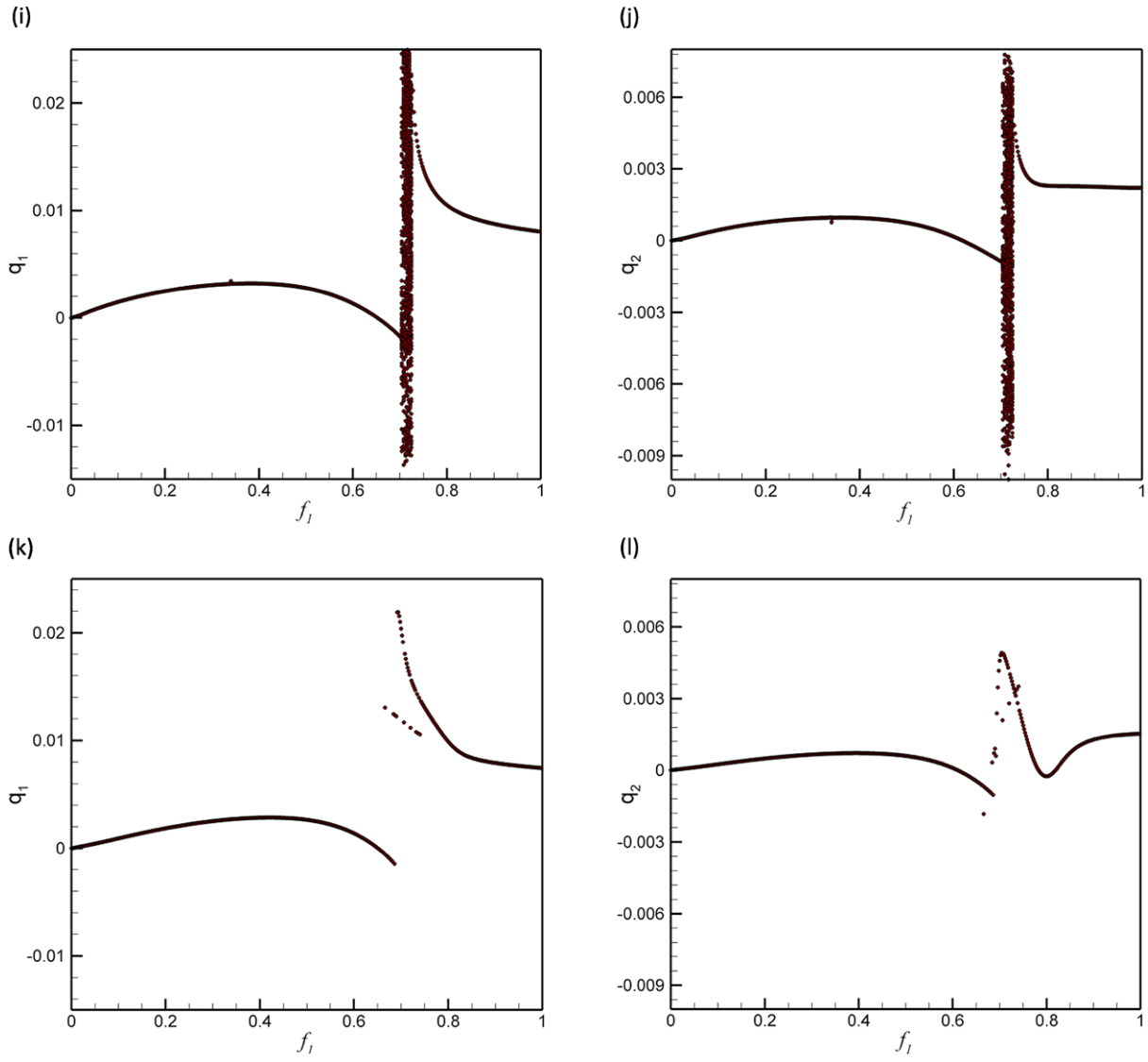

Fig. 10 (*Continued*)

$$+\hat{F}(x)\cos(\omega t)=0, \tag{8}$$

with the boundary conditions for a hinged-hinged beam as

$$u|_{x=0}=u|_{x=L}=0, \tag{9}$$

$$w|_{x=0}=\left.\frac{\partial^2 w}{\partial x^2}\right|_{x=0}=0, \quad w|_{x=L}=\left.\frac{\partial^2 w}{\partial x^2}\right|_{x=L}=0. \tag{10}$$

Neglecting the fast dynamics in the longitudinal direction [36] in (7) and substituting the resulting equation into (8) gives the following:

$$EI\frac{\partial^4 w}{\partial x^4}+\rho A\left(\frac{\partial^2 w}{\partial t^2}+2v\frac{\partial^2 w}{\partial x\partial t}+v^2\frac{\partial^2 w}{\partial x^2}\right) - p\frac{\partial^2 w}{\partial x^2}+\delta(x-x_s)\left(k_1 w+k_2 w^3\right) = \frac{EA}{2L}\frac{\partial^2 w}{\partial x^2}\int_0^L\left(\frac{\partial w}{\partial x}\right)^2 dx+\hat{F}(x)\cos(\omega t). \tag{11}$$

Introducing dimensionless quantities

$$\eta=\frac{w}{L}, \quad \xi=\frac{x}{L}, \quad \xi_s=\frac{x_s}{L},$$

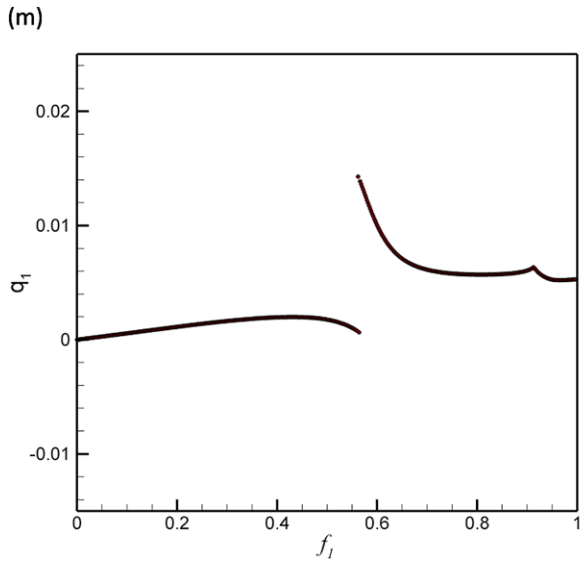

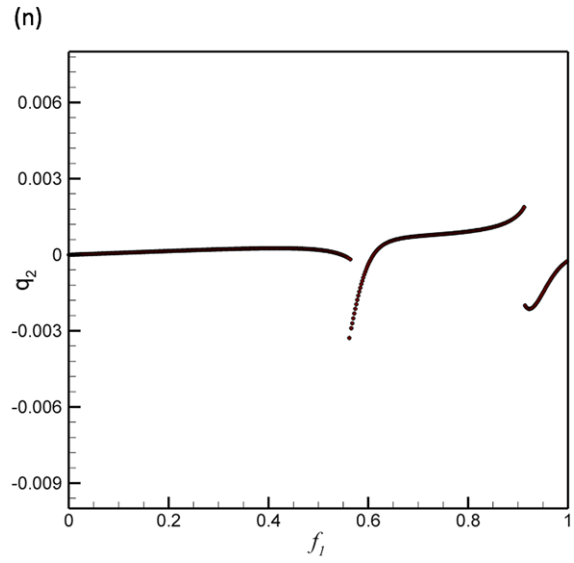

Fig. 10 (*Continued*)

$$\tau = t\sqrt{\frac{p}{\rho AL^2}}, \quad c = v\sqrt{\frac{\rho A}{p}}, \quad v_f = \sqrt{\frac{EI}{pL^2}},$$
$$\alpha = \frac{k_1 L}{p}, \quad \gamma = \frac{k_2 L^3}{p}, \tag{12}$$
$$v_1 = \sqrt{\frac{EA}{p}}F = \frac{\hat{F}L}{p}, \quad \Omega = \omega\sqrt{\frac{\rho AL^2}{p}},$$

the equation of motion can be rewritten as

$$\frac{\partial^2\eta}{\partial\tau^2} + 2c\frac{\partial^2\eta}{\partial\xi\,\partial\tau} + \left(c^2-1\right)\frac{\partial^2\eta}{\partial\xi^2} + v_f^2\frac{\partial^4\eta}{\partial\xi^4} + \delta\left(\xi-\xi_s\right)\left(\alpha\eta+\gamma\eta^3\right) = \frac{1}{2}v_1^2\frac{\partial^2\eta}{\partial\xi^2}\int_0^1\left(\frac{\partial\eta}{\partial\xi}\right)^2 d\xi + F\left(\xi\right)\cos\left(\Omega\tau\right). \tag{13}$$

3 Method of solution

One approach in the vibration analysis of continuous systems is to discretize the partial differential equations of motion to a lower order dimensional system of ordinary differential equations. This is accomplished by using an appropriate spatial representation in terms of a limited number of functions which satisfy the boundary conditions of the system; the linear eigenfunctions are usually employed in vibration problems.

The equation of motion is approximated employing the Galerkin procedure, expanding the transverse displacement $\eta(\xi,\tau)$ in a series of the eigenfunctions of a hinged-hinged beam, i.e.,

$$\eta\left(\xi,\tau\right) = \sum_{r=1}^{N}\phi_r\left(\xi\right)q_r\left(\tau\right). \tag{14}$$

The forcing amplitude is also expressed as

$$F\left(\xi\right) = \sum_{r=1}^{N} f_r\phi_r\left(\xi\right). \tag{15}$$

In the results presented in this paper, only the first mode is excited; only the forcing amplitude associated with the first beam-mode expansion is considered.

Inserting (14) and (15) into (13), multiplying the resulting equation by the corresponding eigenfunction, and integrating with respect to ξ from 0 to 1 gives

$$\sum_{j=1}^{N}\left(\int_0^1\phi_i\phi_j\,d\xi\right)\ddot{q}_j + 2c\sum_{j=1}^{N}\left(\int_0^1\phi_i\phi_j'\,d\xi\right)\dot{q}_j + \left(c^2-1\right)\sum_{j=1}^{N}\left(\int_0^1\phi_i\phi_j''\,d\xi\right)q_j + v_f^2\sum_{j=1}^{N}\left(\int_0^1\phi_i\phi_j''''\,d\xi\right)q_j + \alpha\sum_{j=1}^{N}\left(\int_0^1\delta(\xi-\xi_s)\phi_i\phi_j\,d\xi\right)q_j$$

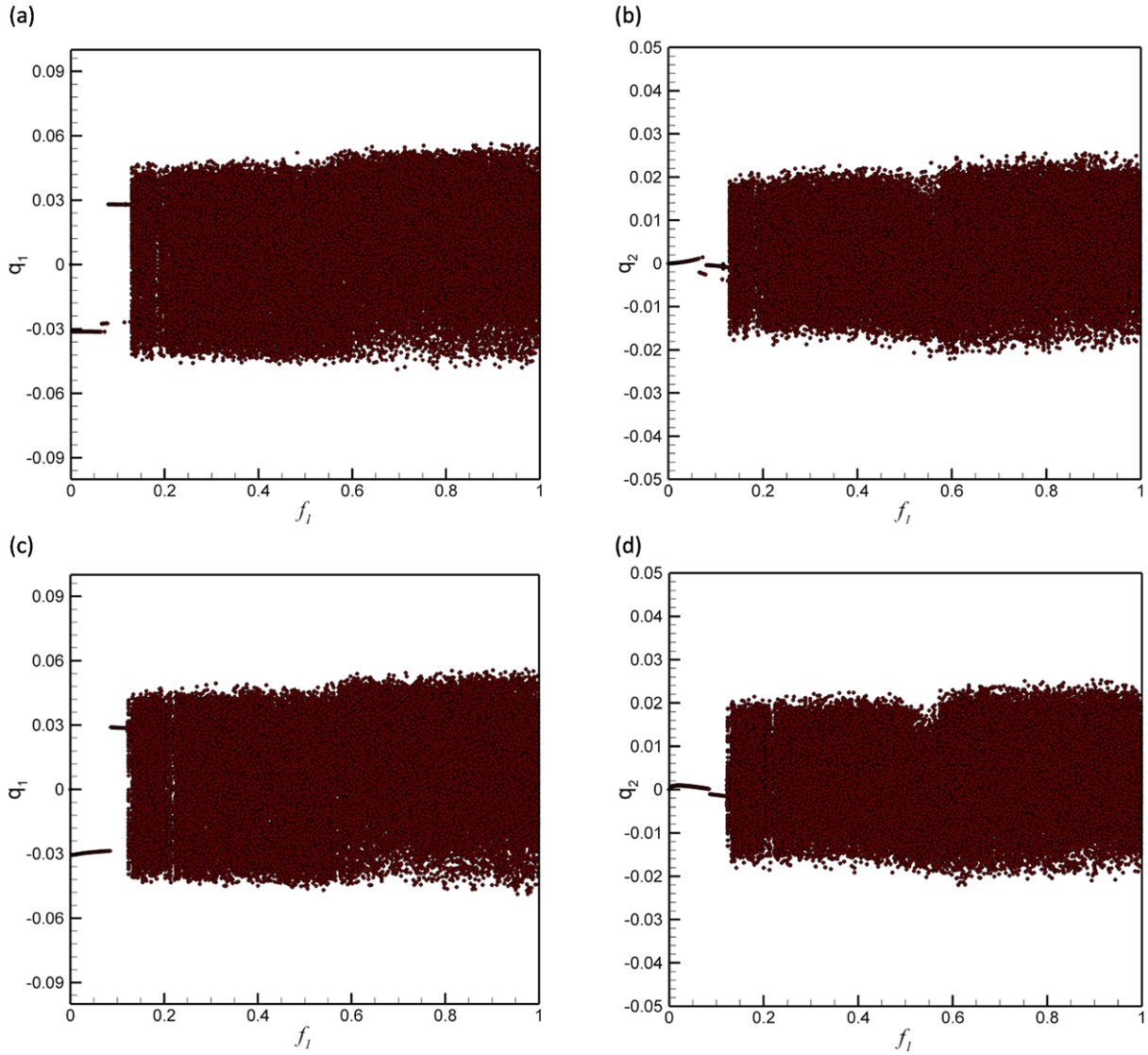

Fig. 11 Bifurcation diagrams of Poincaré points for increasing forcing amplitude on the system. The first and second modes, respectively, with (**a**, **b**) $\alpha = 0$ and $\gamma = 0$, (**c**, **d**) $\alpha = 0.6$ and $\gamma = 0.12$, (**e**, **f**) $\alpha = 1.5$ and $\gamma = 0.3$, (**g**, **h**) $\alpha = 3.0$ and $\gamma = 0.6$, (**i**, **j**) $\alpha = 5.0$ and $\gamma = 1.0$, (**k**, **l**) $\alpha = 7.5$ and $\gamma = 1.5$, and (**m**, **n**) $\alpha = 15$ and $\gamma = 3.0$. The axial speed is set to 2.0

$$+\gamma\sum_{j=1}^{N}\sum_{k=1}^{N}\sum_{l=1}^{N}\left(\int_0^1\delta(\xi-\xi_s)\phi_i\phi_j\phi_k\phi_l\,d\xi\right)\times q_jq_kq_l$$
$$=\frac{1}{2}v_1^2\sum_{j=1}^{N}\sum_{k=1}^{N}\sum_{l=1}^{N}\left(\int_0^1\phi_i\phi_j''\,d\xi\int_0^1\phi_k'\phi_l'\,d\xi\right)q_jq_kq_l+\sum_{j=1}^{N}\left(\int_0^1 f_j\phi_j\phi_i\,d\xi\right)\cos(\Omega\tau),\quad i=1,2,\ldots,N, \tag{16}$$

where dot and prime denote the differentiation with respect to dimensionless time and axial coordinate, respectively.

In order to use direct time integration and the pseudo-arclength continuation technique, (16) is transformed into a set of first order ordinary differential equations using the following transformation:

$$y_i=\dot{q}_i, \tag{17}$$

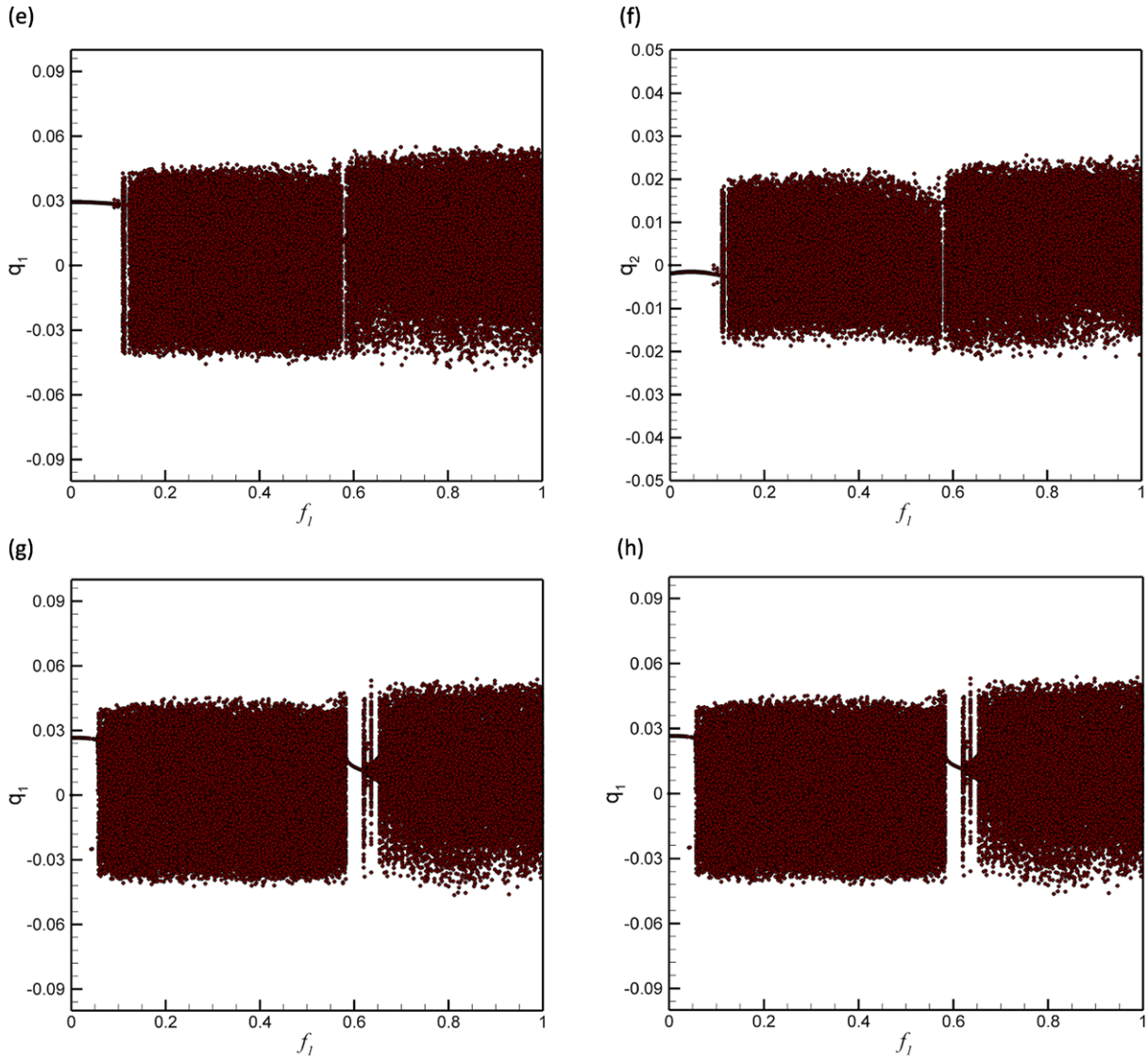

Fig. 11 (*Continued*)

which results in

$$\sum_{j=1}^{N}\left(\int_0^1 \phi_i\phi_j\,d\xi\right)\dot{y}_j + 2c\sum_{j=1}^{N}\left(\int_0^1 \phi_i\phi_j'\,d\xi\right)y_j + \left(c^2-1\right)\sum_{j=1}^{N}\left(\int_0^1 \phi_i\phi_j''\,d\xi\right)q_j + v_f^2\sum_{j=1}^{N}\left(\int_0^1 \phi_i\phi_j''''\,d\xi\right)q_j + \alpha\sum_{j=1}^{N}\left(\int_0^1 \delta(\xi-\xi_s)\phi_i\phi_j\,d\xi\right)q_j + \gamma\sum_{j=1}^{N}\sum_{k=1}^{N}\sum_{l=1}^{N}\left(\int_0^1 \delta(\xi-\xi_s)\phi_i\phi_j\phi_k\phi_l\,d\xi\right) \times q_j q_k q_l = \frac{1}{2}v_1^2\sum_{j=1}^{N}\sum_{k=1}^{N}\sum_{l=1}^{N}\left(\int_0^1 \phi_i\phi_j''\,d\xi\right)$$

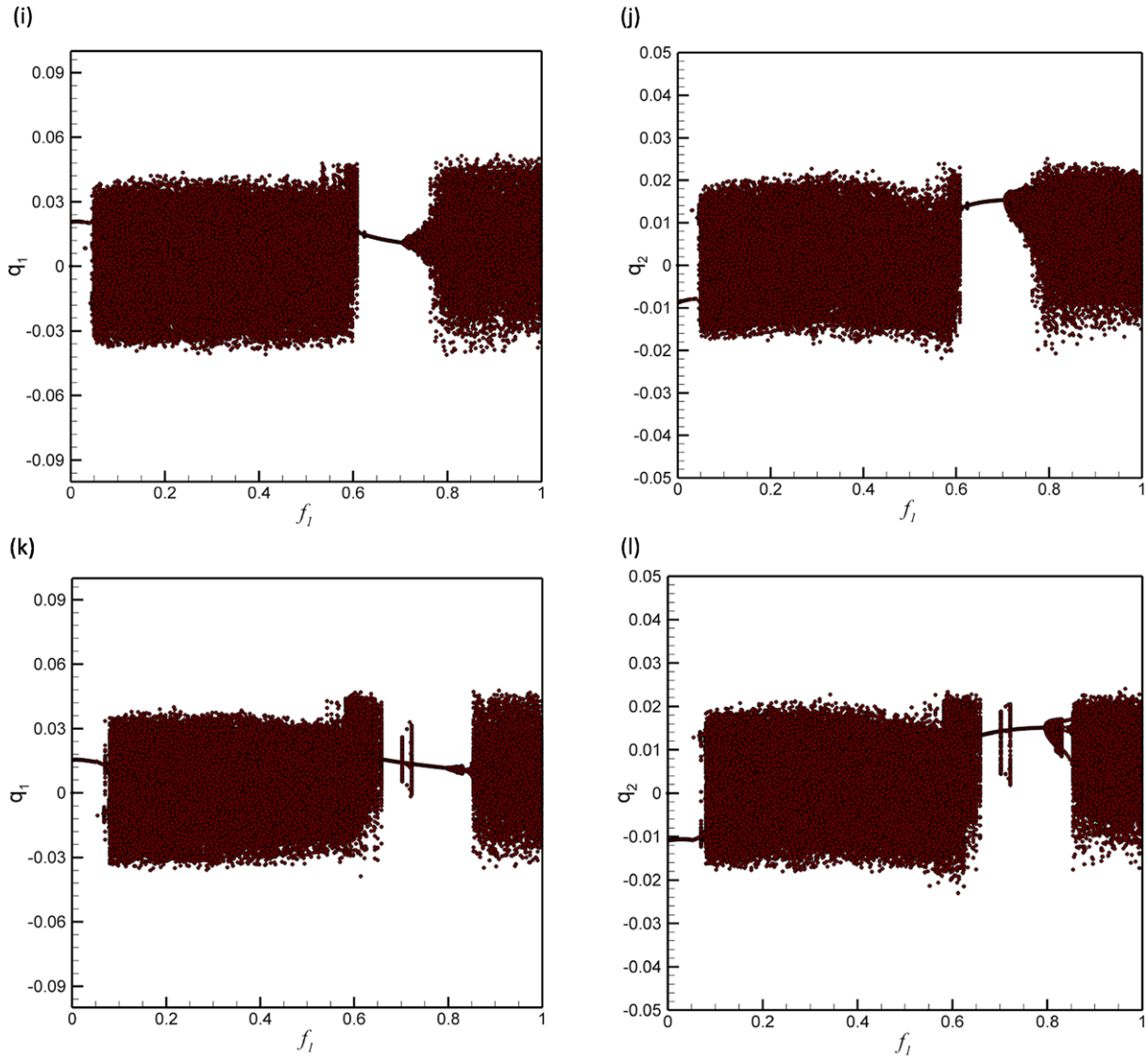

Fig. 11 (*Continued*)

$$\times \int_0^1 \phi_k' \phi_l' \, d\xi \Big) q_j q_k q_l + \sum_{j=1}^{N} \Big(\int_0^1 f_j \phi_j \phi_i \, d\xi \Big) \cos(\Omega \tau), \quad i = 1, 2, \ldots, N. \tag{18}$$

Equations (17) and (18) form $2N$ non-linear ordinary differential equations which are solved numerically choosing $N = 6$ (totalling 12 coupled non-linear first-order ordinary differential equations). In particular, the variable step-size Runge-Kutta method along with the pseudo-arclength continuation technique [55] are adopted, yielding time-varying or static generalised coordinates. It should also be mentioned that the numerical simulations include viscous damping μ.

4 Amplitude-frequency responses

In this section, the amplitude-frequency response of the system is plotted for several values of system parameters. First, the response of the system away from internal resonances, the type of bifurcations, and sta-

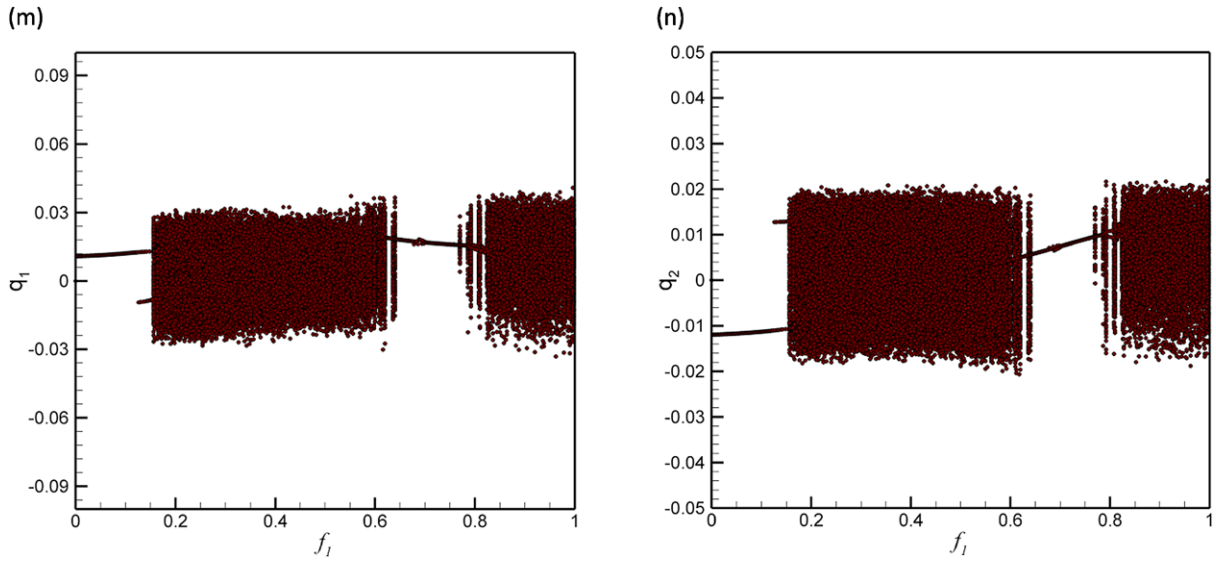

Fig. 11 (*Continued*)

bility of solution branches are examined. Second, the effect of the system parameters on the response is investigated. Lastly, the response of the system near an internal resonance is examined.

The amplitude of the first generalised coordinate is presented in Fig. 2 for the harmonic excitation amplitude $f_1 = 0.0055$ and $f_i = 0 (i = 2, 3, \ldots, 6)$ in the neighbourhood of the fundamental natural frequency. Other dimensionless parameters associated with Fig. 2 are the following: $c = 0.2$, $v_f = 0.173$, $v_1 = 33.526$, $\mu = 0.04$, $\alpha = 1.5$, $\gamma = 0.3$, and, $\xi_s = 0.3$. This plot shows that the type of non-linearity is hardening; as the excitation frequency is increased from $\Omega = 0.6\omega_1$, the response amplitude, which is stable, increases accordingly until the first limit point at A, where $\Omega = 1.4101\omega_1$. As the excitation frequency is slightly decreased, the response becomes unstable until the second limit point is reached at point B, where $\Omega = 1.0547\omega_1$; the stability is regained at this point.

In order to characterise the effect of system parameters on the amplitude-frequency response, these diagrams are plotted in Figs. 3–8 for the system with several system parameters and away from internal resonances. From these figures, the following conclusions may be drawn: (i) as v_1 is increased, the curve bends more to the right, and hence the hardening behaviour becomes stronger, as seen in Fig. 3; (ii) as seen in Fig. 4, increasing the forcing amplitude causes the response amplitude to increase; (iii) as the axial speed is increased from 0.1 to 0.5, the multi-valued region of the response becomes wider (Fig. 5); (iv) as the viscous damping is increased, the response amplitude decreases, as shown in Fig. 6; (v) as seen in Fig. 7, although the linear and non-linear stiffness coefficients of the spring affect the system response significantly, it is difficult to draw any conclusion regarding the trend of the influence; (vi) changing the spring location from the left end to the mid-point results in a decrease in the hardening-type behaviour of the system, as seen in Fig. 8.

Shown in Fig. 9 is the typical dynamics of the system possessing a three-to-one internal resonance with the following dimensionless parameters: $c = 0.7025$, $v_f = 0.173$, $v_1 = 10$, $\mu = 0.03$, $f_1 = 0.0055$, $f_i = 0$ $(i = 2, 3, 4, 5, 6)$, $\alpha = 3.5$, $\gamma = 0.7$, and $\xi_s = 0.2$. With these parameters, a three-to-one internal resonance occurs; i.e. $\omega_2 \approx 3\omega_1$. As seen in Fig. 9(a, b), energy is transferred from the external excitation to the first (excited) mode. A portion of the energy gained is then transferred to the second mode, as seen in Fig. 9(b).

5 Bifurcation diagrams

The bifurcation diagrams of Poincaré maps of the system, when either the forcing amplitude or the axial speed is increased, are obtained for several values of the spring stiffness coefficients. This is accomplished

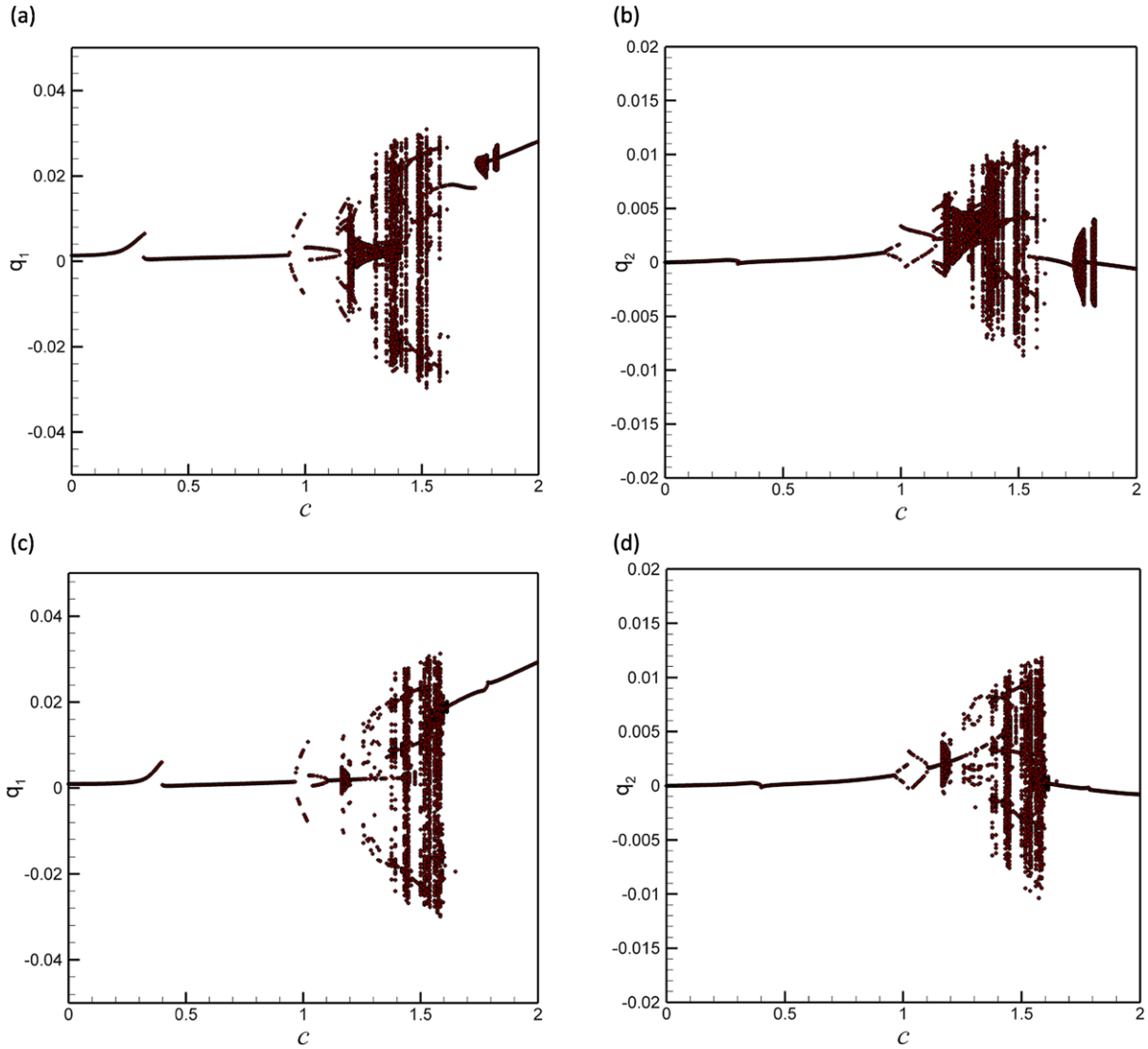

Fig. 12 Bifurcation diagrams of Poincaré points for increasing axial speed of the system. The first and second modes, respectively, with (**a**, **b**) $\alpha = 0$ and $\gamma = 0$, (**c**, **d**) $\alpha = 0.6$ and $\gamma = 0.12$, (**e**, **f**) $\alpha = 1.5$ and $\gamma = 0.3$, (**g**, **h**) $\alpha = 3.0$ and $\gamma = 0.6$, (**i**, **j**) $\alpha = 5.0$ and $\gamma = 1.0$, (**k**, **l**) $\alpha = 7.5$ and $\gamma = 1.5$, (**m**, **n**) $\alpha = 15$ and $\gamma = 3.0$, and (**l**, **o**) $\alpha = 30$ and $\gamma = 6.0$

via direct time integration of (17) and (18) using a variable step-size Runge–Kutta method. Although the AUTO code is capable of providing continuation of solutions and stability and bifurcation analysis using the pseudo-arclength continuation scheme and collocation methods, it is not able to obtain quasi-periodic and chaotic motions. This restriction is overcome here using direct time integration. Two system parameters, namely the forcing amplitude and axial speed, are chosen as bifurcation parameters and the phase space was sectioned in every period of the exciting force. The computer codes were run for a time interval of [0 2500] dimensionless seconds and the last 30% of the response has been retained, excluding any possible transient effects. All the results presented in this section have been obtained using the generalised coordinates for a given value of the bifurcation parameter as initial conditions for the next value. In this section, by saying *response*, the q_1 motion is meant, and amplitude means the amplitude of the q_1 motion where it is sectioned. The excitation frequency is set to 1.2.

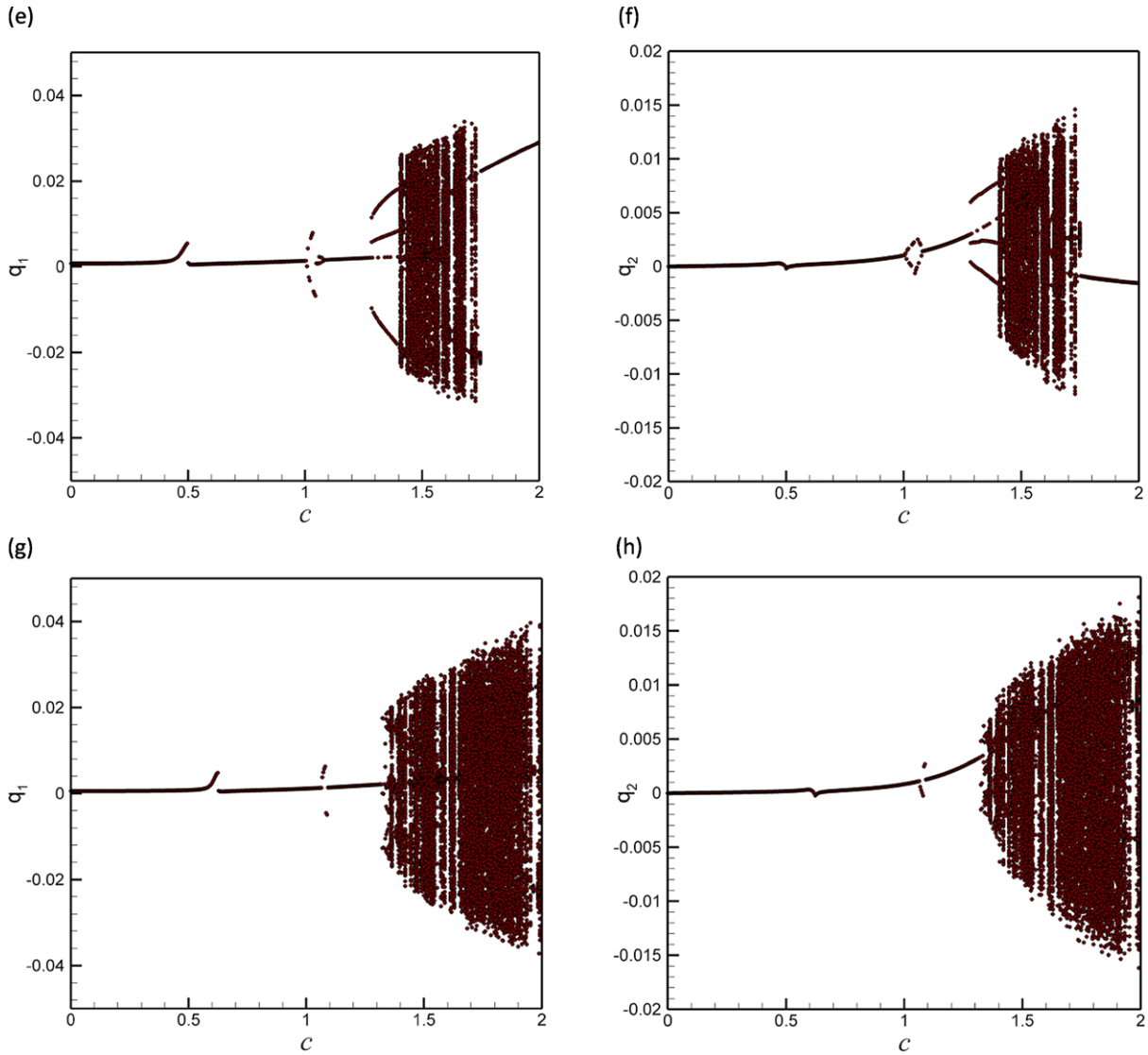

Fig. 12 (*Continued*)

The bifurcation diagrams of the first two generalised coordinates versus the magnitude of the external force are shown in Fig. 10(a, b)–(m, n), respectively, for the spring stiffness coefficients of (i) $\alpha = 0$ and $\gamma = 0$, (ii) $\alpha = 0.6$ and $\gamma = 0.12$, (iii) $\alpha = 1.5$ and $\gamma = 0.3$, (iv) $\alpha = 3.0$ and $\gamma = 0.6$, (v) $\alpha = 5.0$ and $\gamma = 1.0$, (vi) $\alpha = 7.5$ and $\gamma = 1.5$, and (vii) $\alpha = 15.0$ and $\gamma = 3.0$, respectively. The other dimensionless parameters of the system of Fig. 10 are the following: $c = 0.7$, $v_f = 0.173$, $v_1 = 33.526$, $\mu = 0.04$, and $\xi_s = 0.4$. The bifurcation diagram of the system with $\alpha = \gamma = 0$, i.e. case (i), is shown in Fig. 10(a, b). As seen in Fig. 10(a), as the forcing amplitude is increased, the response amplitude increases initially, then decreases until a sudden jump occurs at $f_1 = 0.132$. The motion becomes quasi-periodic in the forcing amplitude range of [0.316 0.324]. There are two co-existing attractors in the interval of [0.344 0.424] and the response repeatedly jumps from one to the other. As the forcing amplitude is increased slightly, the system returns to its original period and maintains it until $f_1 = 0.488$ is hit, where the motion becomes period-3. In the forcing amplitude range of [0.488 0.598], the response repeatedly becomes periodic and period-3. The period is re-

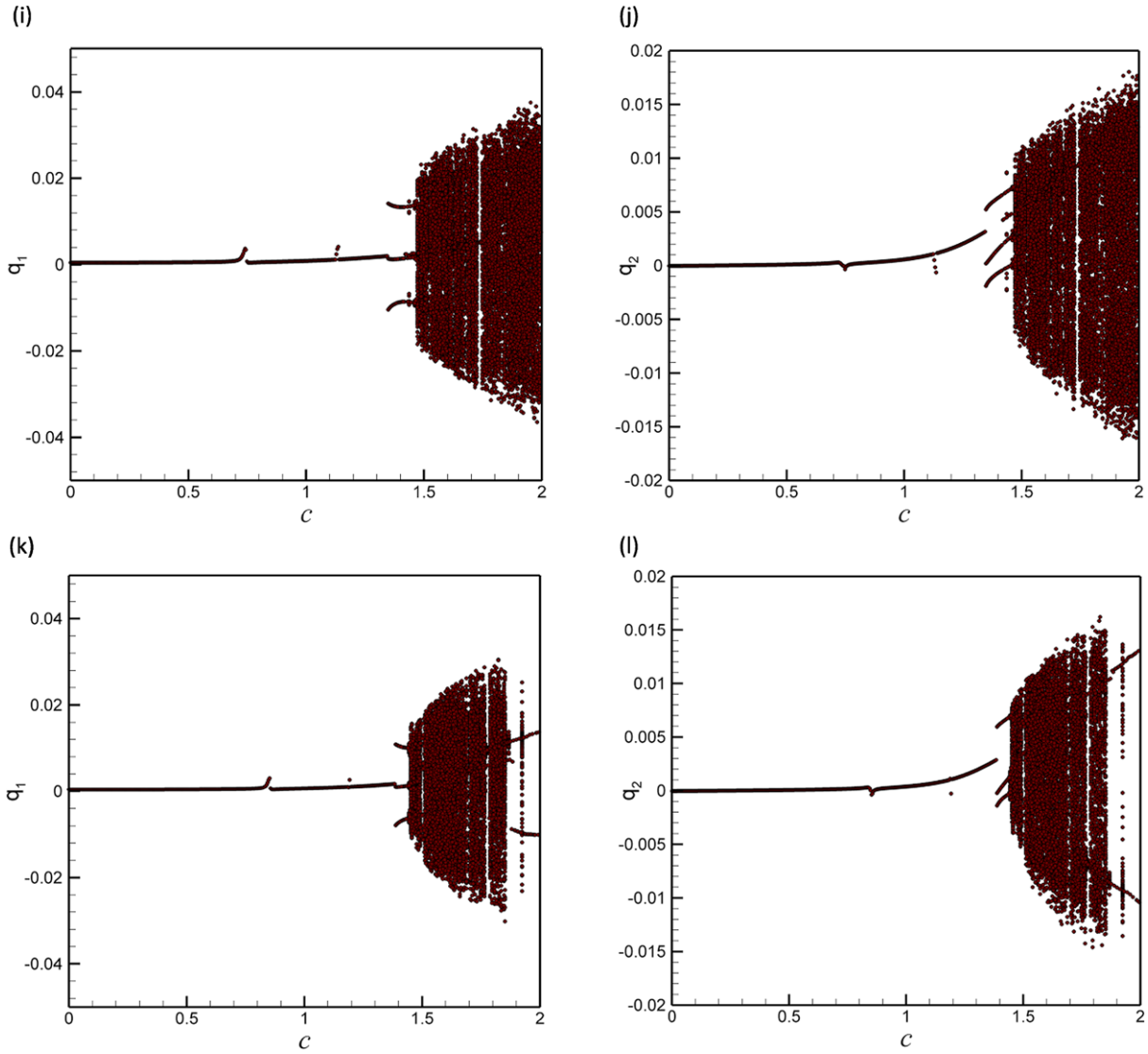

Fig. 12 (*Continued*)

gained at $f_1 = 0.600$ and maintained until $f_1 = 0.694$. The motion becomes quasi-periodic in the interval [0.696 0.706], periodic in [0.708 .748], quasi-periodic at $f_1 = 0.750$, period-5 in the interval [0.752 0.756], and quasi-periodic in the range of [0.758 0.776]. The motion regains the period at $f_1 = 0.778$ which is characterised by a jump (an increase in the amplitude) and maintains that period until $f_1 = 0.934$, where it becomes period-3. Beyond this forcing amplitude until $f_1 = 1.00$, there are two attractors, one periodic and the other period-3; the motion repeatedly jumps from one to the other.

Figure 10(c, d) shows the bifurcation diagrams for the system with $\alpha = 0.6$ and $\gamma = 0.12$ (i.e. in the presence of the intermediate spring-support). As seen in this figure, adding an intermediate spring-support with the above-mentioned stiffness coefficients does not change the system dynamics substantially. The bifurcation diagrams for the system with $\alpha = 1.5$ and $\gamma = 0.3$ is shown in Fig. 10(e, f), where a spring stiffer than that of the previous case (Fig. 10(c, d)) is used. Investigating the dynamics of the system with higher spring stiffness, specifically with $\alpha = 3.0$ and $\gamma = 0.6$ (Fig. 10(g, h)), $\alpha = 5.0$ and $\gamma = 1.0$ (Fig. 10(i, j)),

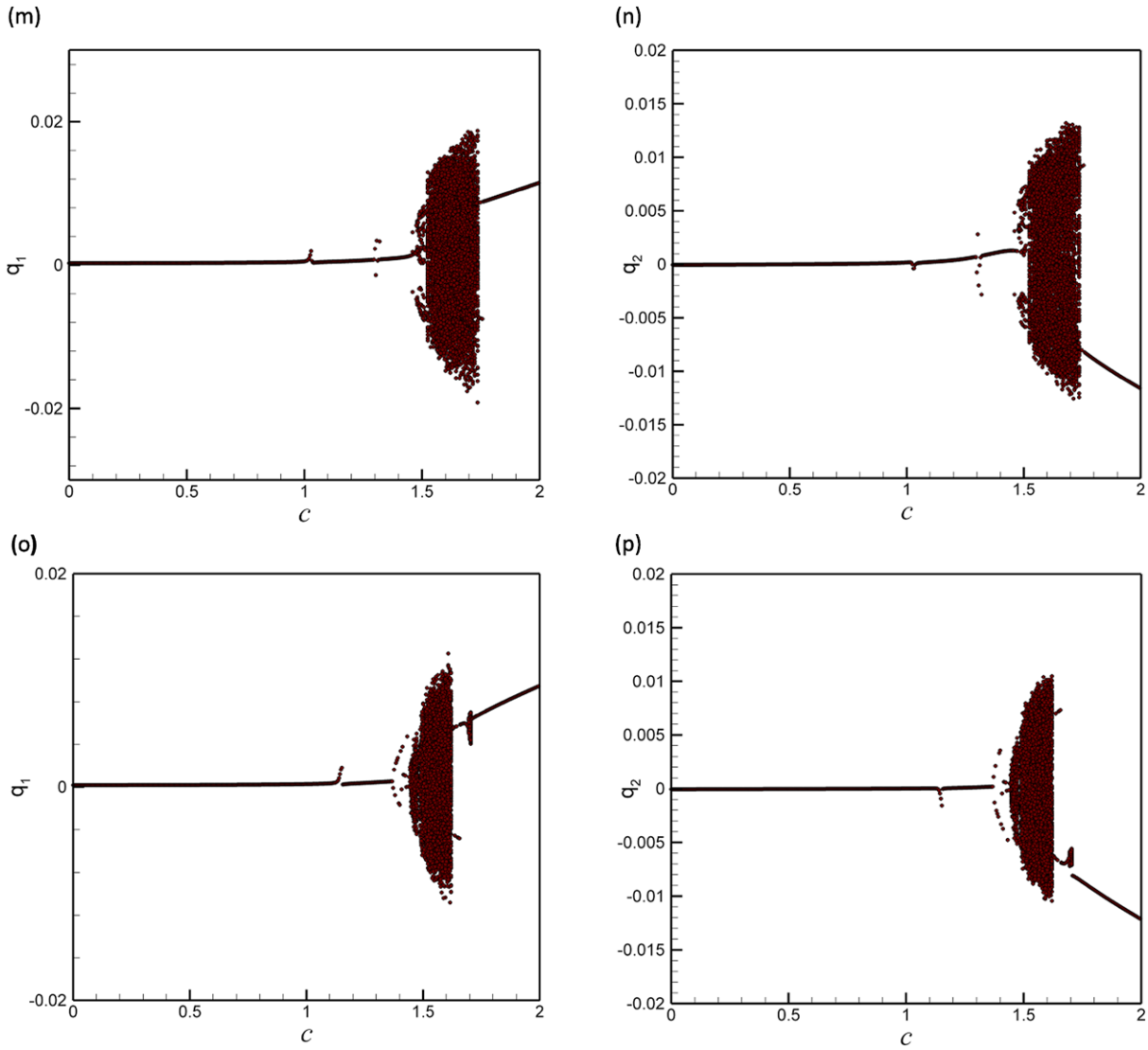

Fig. 12 (*Continued*)

$\alpha = 7.5$ and $\gamma = 1.5$ (Fig. 10(k, l)), and $\alpha = 15.0$ and $\gamma = 3.0$ (Fig. 10(m, n)) reveals that, in general, due to an increased stiffness coefficient of the spring-support, the cascade of higher order bifurcations as well as coexisting and strange attractors disappear; a stiffer spring-support stabilises the system.

The bifurcation diagram of the same system shown in Fig. 10(a–n), but with a higher axial speed, i.e., $c = 2.0$, are plotted in Fig. 11(a–n), again for different values of the spring stiffness. As seen in Fig. 11(a) for q_1, in general, the motion is periodic at first, then undergoes some small jumps, and finally becomes chaotic. The bifurcation diagrams of the system with higher spring stiffness are shown in Figs. 11(c, d), 11(e, f), 11(g, h), 11(i, j), 11(k, l), and 11(m, n), respectively; Fig. 11(a, b) has no spring, and Fig. 11(m, n) has the strongest one. From comparison of the system dynamics in these figures, one may conclude that the range of chaotic regions decreases as the stiffness coefficient of the spring is increased; the fully chaotic region in Fig. 11(a, b) is split into two regions, separated by a simpler kind of attractor, such as periodic or quasi-periodic (Fig. 11(g–n)).

In Fig. 12(a–p), the axial speed is varied as the control parameter for different spring stiffness coefficients. The following system parameters have been selected for Fig. 12(a–p): $f_1 = 0.06$, $v_f = 0.173$, $v_1 = 33.526$, $\mu = 0.04$, and $\xi_s = 0.4$. As seen in this figure, it is hard to draw any general conclusion regarding the effect of the spring stiffness on the bifurcation diagrams of the system. One of the cases with the most interesting dynamics is explained in detail in the following. As seen in Fig. 12(e), the amplitude of q_1 jumps at $c = 0.500$. There are two coexisting attractors in the axial speed range of [1.008 1.076], where the response jumps repeatedly from one to the other. As the axial speed is increased further, the motion becomes period-3 at $c = 1.284$, and continues until $c = 1.404$, except for some c values, where the motion is periodic. The motion becomes chaotic at $c = 1.408$; more specifically, in the interval [1.408 1.748] there are four attractors, namely chaotic, quasi-periodic, period doubling, and periodic. These attractors are repeated one after another, as the response jumps between them. Finally, the motion regains the period at $c = 1.752$.

6 Conclusions

Non-linear vibration characteristics of an axially moving beam supported by an intermediate spring has been studied by means of the pseudo-arclength continuation technique for continuation and bifurcation analysis of non-linear ordinary differential equations, as well as direct time integration via the variable step-size Runge–Kutta method. The results for both cases, with and without a three-to-one internal resonance have been presented. For different spring-support coefficients, the system displays very rich dynamical behaviour involving periodic, quasi-periodic, period-2, period-3, and chaotic motions. In connection with the sub-critical dynamics, the system away from an internal resonance displays two limit point bifurcations; between these the solution branch is unstable.

It is hoped that the results presented in this paper are helpful toward a better understanding of the dynamics of an axially moving beam with an intermediate spring-support, specifically the effect of spring stiffness on the dynamics of the system, particularly those which are hard to investigate via analytical techniques.

References

1. Swope, R.D., Ames, W.F.: Vibrations of a moving threadline. J. Franklin Inst. **275**, 36–55 (1963)
2. Wickert, J., Mote, C.D.J.: Current research on the vibration and stability of moving materials. Shock Vib. Dig. **20**, 3–13 (1988)
3. Mote, J.: On the nonlinear oscillation of an axially moving string. J. Appl. Mech. **33**, 463–464 (1966)
4. Naguleswaran, S., Williams, C.J.H.: Lateral vibration of band-saw blades, pulley belts and the like. Int. J. Mech. Sci. **10**, 239–250 (1968)
5. Thurman, A.L., Mote, C.D.J.: Free, periodic, nonlinear oscillation of an axially moving strip. J. Appl. Mech. **36**, 83–91 (1969)
6. Shih, L.Y.: Three-dimensional non-linear vibration of a traveling string. Int. J. Non-Linear Mech. **6**, 427–434 (1971)
7. Simpson, A.: Transverse modes and frequencies of beams translating between fixed end supports. J. Mech. Eng. Sci. **15**, 159–164 (1973)
8. Holmes, P.J.: Pipes supported at both ends cannot flutter. J. Appl. Mech. **45**, 619–622 (1978)
9. Wickert, J.A., Mote, J.C.D.: Classical vibration analysis of axially moving continua. J. Appl. Mech. **57**, 738–744 (1990)
10. Wickert, J.A., Mote, J.C.D.: Travelling load response of an axially moving string. J. Sound Vib. **149**, 267–284 (1991)
11. Wickert, J.A.: Non-linear vibration of a traveling tensioned beam. Int. J. Non-Linear Mech. **27**, 503–517 (1992)
12. Öz, H.R., Pakdemirli, M., Özkaya, E.: Transition behaviour from string to beam for an axially accelerating material. J. Sound Vib. **215**, 571–576 (1998)
13. Pakdemirli, M., Özkaya, E.: Approximate boundary layer solution of a moving beam problem. Math. Comput. Appl. **3**, 93–100 (1998)
14. Pakdemirli, M., Ulsoy, A.G.: Stability analysis of an axially accelerating string. J. Sound Vib. **203**, 815–832 (1997)
15. Pakdemirli, M., Ulsoy, A.G., Ceranoglu, A.: Transverse vibration of an axially accelerating string. J. Sound Vib. **169**, 179–196 (1994)
16. Yuh, J., Young, T.: Dynamic modeling of an axially moving beam in rotation: simulation and experiment. J. Dyn. Syst. Meas. Control **113**, 34–40 (1991)
17. Zhu, W.D., Guo, B.Z.: Free and forced vibration of an axially moving string with an arbitrary velocity profile. J. Appl. Mech. **65**, 901–907 (1998)
18. Chakraborty, G., Mallik, A.K.: Non-Linear vibration of a travelling beam having an intermediate guide. Nonlinear Dyn. **20**, 247–265 (1999)
19. Zhang, L., Zu, J.W.: Nonlinear vibration of parametrically excited viscoelastic moving belts, Part II: Stability analysis. J. Appl. Mech. **66**, 403–409 (1999)
20. Tan, C.A., Yang, B., Mote, J.C.D.: Dynamic response of an axially moving beam coupled to hydrodynamic bearings. J. Vib. Acoust. **115**, 9–15 (1993)
21. Marynowski, K.: Free vibration analysis of the axially moving Levy-type viscoelastic plate. Eur. J. Mech. A, Solids **29**, 879–886 (2010)
22. Marynowski, K.: Two-dimensional rheological element in modelling of axially moving viscoelastic web. Eur. J. Mech. A, Solids **25**, 729–744 (2006)

23. Marynowski, K.: Non-linear vibrations of an axially moving viscoelastic web with time-dependent tension. Chaos Solitons Fractals **21**, 481–490 (2004)
24. Marynowski, K., Kapitaniak, T.: Zener internal damping in modelling of axially moving viscoelastic beam with time-dependent tension. Int. J. Non-Linear Mech. **42**, 118–131 (2007)
25. Marynowski, K., Kapitaniak, T.: Kelvin-Voigt versus Bürgers internal damping in modeling of axially moving viscoelastic web. Int. J. Non-Linear Mech. **37**, 1147–1161 (2002)
26. Chen, L.-Q., Yang, X.-D.: Steady-state response of axially moving viscoelastic beams with pulsating speed: comparison of two nonlinear models. Int. J. Solids Struct. **42**, 37–50 (2005)
27. Chen, L.-Q.: The energetics and the stability of axially moving strings undergoing planar motion. Int. J. Eng. Sci. **44**, 1346–1352 (2006)
28. Chen, L.-Q., Yang, X.-D.: Vibration and stability of an axially moving viscoelastic beam with hybrid supports. Eur. J. Mech. A, Solids **25**, 996–1008 (2006)
29. Chen, L.-Q., Zhao, W.-J.: A conserved quantity and the stability of axially moving nonlinear beams. J. Sound Vib. **286**, 663–668 (2005)
30. Chen, L.-Q., Zhao, W.-J., Zu, J.W.: Simulations of transverse vibrations of an axially moving string: a modified difference approach. Appl. Math. Comput. **166**, 596–607 (2005)
31. Tang, Y.-Q., Chen, L.-Q., Yang, X.-D.: Natural frequencies, modes and critical speeds of axially moving Timoshenko beams with different boundary conditions. Int. J. Mech. Sci. **50**, 1448–1458 (2008)
32. Tang, Y.-Q., Chen, L.-Q., Yang, X.-D.: Parametric resonance of axially moving Timoshenko beams with time-dependent speed. Nonlinear Dyn. **58**, 715–724 (2009)
33. Tang, Y.-Q., Chen, L.-Q., Yang, X.-D.: Nonlinear vibrations of axially moving Timoshenko beams under weak and strong external excitations. J. Sound Vib. **320**, 1078–1099 (2009)
34. Yang, X.-D., Tang, Y.-Q., Chen, L.-Q., Lim, C.W.: Dynamic stability of axially accelerating Timoshenko beam: averaging method. Eur. J. Mech. A, Solids **29**, 81–90 (2010)
35. Chen, L.-Q., Chen, H., Lim, C.W.: Asymptotic analysis of axially accelerating viscoelastic strings. Int. J. Eng. Sci. **46**, 976–985 (2008)
36. Pellicano, F., Vestroni, F.: Nonlinear dynamics and bifurcations of an axially moving beam. J. Vib. Acoust. **122**, 21–30 (2000)
37. Suweken, G., Van Horssen, W.T.: On the weakly nonlinear, transversal vibrations of a conveyor belt with a low and time-varying velocity. Nonlinear Dyn. **31**, 197–223 (2003)
38. Huang, J.L., Su, R.K.L., Li, W.H., Chen, S.H.: Stability and bifurcation of an axially moving beam tuned to three-to-one internal resonances. J. Sound Vib. **330**, 471–485 (2011)
39. Ghayesh, M.H.: Stability characteristics of an axially accelerating string supported by an elastic foundation. Mech. Mach. Theory **44**, 1964–1979 (2009)
40. Ghayesh, M.H.: Parametric vibrations and stability of an axially accelerating string guided by a non-linear elastic foundation. Int. J. Non-Linear Mech. **45**, 382–394 (2010)
41. Ghayesh, M.H.: Nonlinear transversal vibration and stability of an axially moving viscoelastic string supported by a partial viscoelastic guide. J. Sound Vib. **314**, 757–774 (2008)
42. Ghayesh, M.H.: On the natural frequencies, complex mode functions, and critical speeds of axially traveling laminated beams: parametric study. Acta Mech. Solida Sin. **24**(4), 373–382 (2011)
43. Ghayesh, M.H., Balar, S.: Non-linear parametric vibration and stability of axially moving visco-elastic Rayleigh beams. Int. J. Solids Struct. **45**, 6451–6467 (2008)
44. Ghayesh, M.H., Balar, S.: Non-linear parametric vibration and stability analysis for two dynamic models of axially moving Timoshenko beams. Appl. Math. Model. **34**, 2850–2859 (2010)
45. Ghayesh, M.H., Moradian, N.: Nonlinear dynamic response of axially moving, stretched viscoelastic strings. Arch. Appl. Mech. **81**, 781–799 (2011)
46. Ghayesh, M.H., Yourdkhani, M., Balar, S., Reid, T.: Vibrations and stability of axially traveling laminated beams. Appl. Math. Comput. **217**, 545–556 (2010)
47. Sahebkar, S.M., Ghazavi, M.R., Khadem, S.E., Ghayesh, M.H.: Nonlinear vibration analysis of an axially moving drillstring system with time dependent axial load and axial velocity in inclined well. Mech. Mach. Theory **46**, 743–760 (2011)
48. Ghayesh, M.H., Païdoussis, M.P.: Three-dimensional dynamics of a cantilevered pipe conveying fluid, additionally supported by an intermediate spring array. Int. J. Non-Linear Mech. **45**, 507–524 (2010)
49. Ghayesh, M.H., Païdoussis, M.P.: Dynamics of a fluid-conveying cantilevered pipe with intermediate spring support. ASME Conf. Proc. 893–902 (2010)
50. Ghayesh, M.H., Païdoussis, M.P., Modarres-Sadeghi, Y.: Three-dimensional dynamics of a fluid-conveying cantilevered pipe fitted with an additional spring-support and an end-mass. J. Sound Vib. **330**, 2869–2899 (2011)
51. Ghayesh, M.H., Kazemirad, S., Darabi, M.A.: A general solution procedure for vibrations of systems with cubic nonlinearities and nonlinear/time-dependent internal boundary conditions. J. Sound Vib. **330**(22), 5382–5400 (2011)
52. Ghayesh, M.H., Kazemirad, S., Darabi, M.A., Woo, P.: Thermo-mechanical nonlinear vibration analysis of a spring-mass-beam system. Arch. Appl. Mech. (2011). doi:10.1007/s00419-011-0558-4
53. Ghayesh, M.H., Alijani, F., Darabi, M.A.: An analytical solution for nonlinear dynamics of a viscoelastic beam-heavy mass system. J. Mech. Sci. Technol., **25**(8), 1915–1923 (2011)
54. Darabi, M.A., Kazemirad, S., Ghayesh, M.H.: Free vibrations of beam-mass-spring systems: analytical analysis with numerical confirmation. Acta Mech. Sin. (2011, in press)
55. Doedel, E.J., Champneys, A.R., Fairgrieve, T.F., Kuznetsov, Y.A., Sandstede, B., Wang, X.: AUTO 97: continuation and bifurcation software for ordinary differential equations (with HomCont). Concordia University, Montreal, Canada (1998)